

## A new damage index for seismic fragility analysis of reinforced concrete columns

Jun Won Kang<sup>1a</sup> and Jeeho Lee<sup>\*2</sup>

<sup>1</sup>Department of Civil Engineering, Hongik University, Seoul, 04066, Korea

<sup>2</sup>Department of Civil and Environmental Engineering, Dongguk University, Seoul, 04620, Korea

(Received August 8, 2016, Revised October 3, 2016, Accepted October 5, 2016)

**Abstract.** A new structural damage index for seismic fragility analysis of reinforced concrete columns is developed based on a local tensile damage variable of the Lee and Fenves plastic-damage model. The proposed damage index is formulated from the nonlinear regression of experimental column test data. In contrast to the response-based damage index, the proposed damage index is well-defined in the form of a single monotonically-increasing function of the volume weighted average of local damage distribution, and provides the necessary computability and objectivity. It is shown that the present damage index can be appropriately zoned to be used in seismic fragility analysis. An application example in the computational seismic fragility evaluation of reinforced concrete columns validates the effectiveness of the proposed damage index.

**Keywords:** damage index; plastic-damage model; local damage variable; seismic fragility analysis; reinforced concrete column

---

### 1. Introduction

Damage indices enable the quantification of the overall structural damage caused by extreme loading. Those indices can be used to define damage states (Jiang, Chen *et al.* 2011, Liang, Wen *et al.* 2011) and to determine the structural fragility (Shinozuka and Deodatis 1991, Dumova-Jovanoska 2000, Andre, Beale *et al.* 2015). During the last decades, significant advancement has been achieved for the development of damage indices based on the external response of structures subjected to earthquake (Teran-Gilmore and Jirsa 2005, Vielma, Barbat *et al.* 2008, Sinha and Shiradhonkar 2012, Hadzima-Nyarko, Morić *et al.* 2014, Azhdary and Shabakhty 2014). Among the response-based damage indices, one of the most widely used in earthquake engineering is the damage index by Park and Ang (1985), which was derived from a large amount of experimental test data of reinforced concrete columns.

In spite of their popularity, the objectivity of response-based damage indices including Park and Ang's one is not assured because of ambiguity in determining their basis parameter values, such as ultimate displacement and yield strength. This may cause different index calculation results for the

---

\*Corresponding author, Professor, E-mail: [jeeholee@dgu.edu](mailto:jeeholee@dgu.edu)

<sup>a</sup>Assistant Professor, Ph.D., E-mail: [jwkang@hongik.ac.kr](mailto:jwkang@hongik.ac.kr)

same single set of test data. Moreover, this group of damage indices is limited to be applied in computational seismic fragility evaluation because it requires to compute, *a priori*, the ultimate displacement, which can hardly be obtained even by state-of-the-art numerical simulation tools due to its strong nonlinearity on cyclic and dynamic response of a severely damaged reinforced concrete structure. To overcome those shortcomings of the response-based damage index, local-damage-based models have been introduced. A damage-state evaluation method based on two index functions of local damage variables was suggested by Koh, Lee *et al.* (2003). Amziane and Dubé (2008) proposed a global damage index based on local material damages computed by the uniaxial multi-layered element analysis. Nevertheless, most of the developed local-damage-based damage indices, including the aforementioned two, are not in the form of a monotonically-increasing function calibrated to experimental data, which is highly desirable in the context of fragility function.

In this paper, a new structural damage index for seismic fragility analysis of reinforced concrete columns is developed based on a local tensile damage variable of the Lee and Fenves plastic-damage model. The proposed damage index is formulated from the nonlinear regression of experimental column test data. After reviewing the Park and Ang damage index and discussing its non-objectivity in Section 2, the Lee and Fenves plastic-damage model and a reinforced concrete column model in the context of finite element analysis are outlined in Section 3. Then, the procedure for deriving the newly-proposed damage index formulation is described. To validate the effectiveness of the proposed damage index, an application example in the computational seismic fragility evaluation of reinforced concrete columns is presented.

## 2. Park and Ang damage index for reinforced concrete columns

### 2.1 Park and Ang damage index and damage states

One of the most widely used damage indices in seismic damage assessment is the Park and Ang damage index (Park and Ang 1985),  $D_{PA}$ , which uses maximum deformation and cumulative energy dissipated by cyclic loadings. The damage index is expressed as

$$D_{PA} = \frac{\delta_m}{\delta_u} + \beta \frac{E_H}{Q_y \delta_u} \quad (1)$$

where  $\delta_m$  is the maximum displacement in a given cyclic loading,  $\delta_u$  is the ultimate displacement and  $Q_y$  is the yield force under monotonic loading,  $E_H$  is the dissipated hysteretic energy, and  $\beta$  is the non-negative parameter defined as:

$$\beta = (-0.447 + 0.073 \frac{l}{d} + 0.24n_0 + 0.314p_t)(0.7^{\rho_w}) \quad (2)$$

where  $l/d$  is the shear span ratio,  $n_0$  is the normalized axial force of which maximum value is 0.2,  $\rho_w$  is the confinement steel ratio, and  $p_t$  is the longitudinal steel ratio as a percentage.

The Park and Ang damage index can be directly calculated from the results of nonlinear dynamic analysis or experiments. The damage index value can be classified into several damage state zones, which are more practical in seismic fragility analysis. Five damage states and the corresponding ranges in the Park and Ang damage index were suggested by EERI (1994) as shown in Table 1. It is noted that the zoning is applied continuously over the single damage index value.

Table 1 Damage states based on Park and Ang's damage index (EERI, 1994)

Damage index	Damage states				Collapse
	None	Minor	Moderate	Severe	
	0 ~ 0.1	0.1 ~ 0.2	0.2 ~ 0.5	0.5 ~ 1.0	> 1.0

Table 2 Detailed configuration of four reinforced concrete column specimens

Specimens	Axial force $P$ (kN)	Diameter $D$ (mm)	Height $H$ (mm)	Longitudinal reinforcement ratio (%)	Transverse reinforcement ratio (%)	Boundary condition
Column 1	500	500	2250	1.89	0.39	Fixed at one end
Column 2	500	500	2250	1.89	3.21	Fixed at one end
Column 3	490	500	3600	1.20	0.34	Fixed at one end
Column 4	490	500	3600	1.20	0.34	Fixed at both ends

## 2.2 Cyclic column tests and objectivity problem

The quasi-static cyclic loading experiments for four reinforced concrete bridge columns (Koh, Lee *et al.* 2003) are used for the basis data to analyse the Park and Ang damage index and to derive a newly proposed damage index. These columns represent four prototypical configurations of reinforced concrete columns in terms of their slenderness, transverse reinforcement ratio, and boundary condition. Table 2 shows configuration details of the column specimens. Columns 1 and 2 have the same geometric and material configurations except the transverse reinforcement ratio, whose value is 0.39% for Column 1 and 3.21% for Column 2, respectively. Column 3 is longer and more slender than Column 1 with the similar longitudinal and transverse reinforcement ratios. Column 4 has the same configuration as Column 3 except the boundary condition.

Although the Park and Ang damage index has been well accepted owing to its simplicity and the fact that it has been calibrated with a significant amount of observed damage samples, the objectivity of the index is not assured because of the ambiguity in determining the ultimate displacement,  $\delta_u$ , and the yield force,  $Q_y$ , from nonlinear experimental or numerical data. Hence, the damage index can be calculated differently for the same single set of test data, which possibly changes the current damage state. In Fig. 1, the damage state ranges, which are estimated with different readings of  $\delta_u$  and  $Q_y$ , are plotted over the moment versus drift ratio curves of Columns 1 and 2. Specifically, the damage state ranges of Fig. 1(a) and 1(b) were estimated by using two possible ultimate displacement values,  $\delta_u=100$  mm and 140 mm, respectively, from the cyclic test data of Column 1. Fig. 1(c) and 1(d) shows the damage state ranges determined by using  $\delta_u=160$  mm and 200 mm, respectively, for Column 2. The yield force,  $Q_y$ , was 70 kN for all four cases. The figures tell us that, if one used Park and Ang damage index for structural damage evaluation, the damage state ranges could be significantly different according to the values of ultimate displacement used. Park and Ang suggested a method for estimating the ultimate displacement of a member from ductility, flexural displacement, deformation due to bond slip, elastic and inelastic shear deformation (Park and Ang 1985). However, ductility is generally difficult to be estimated,

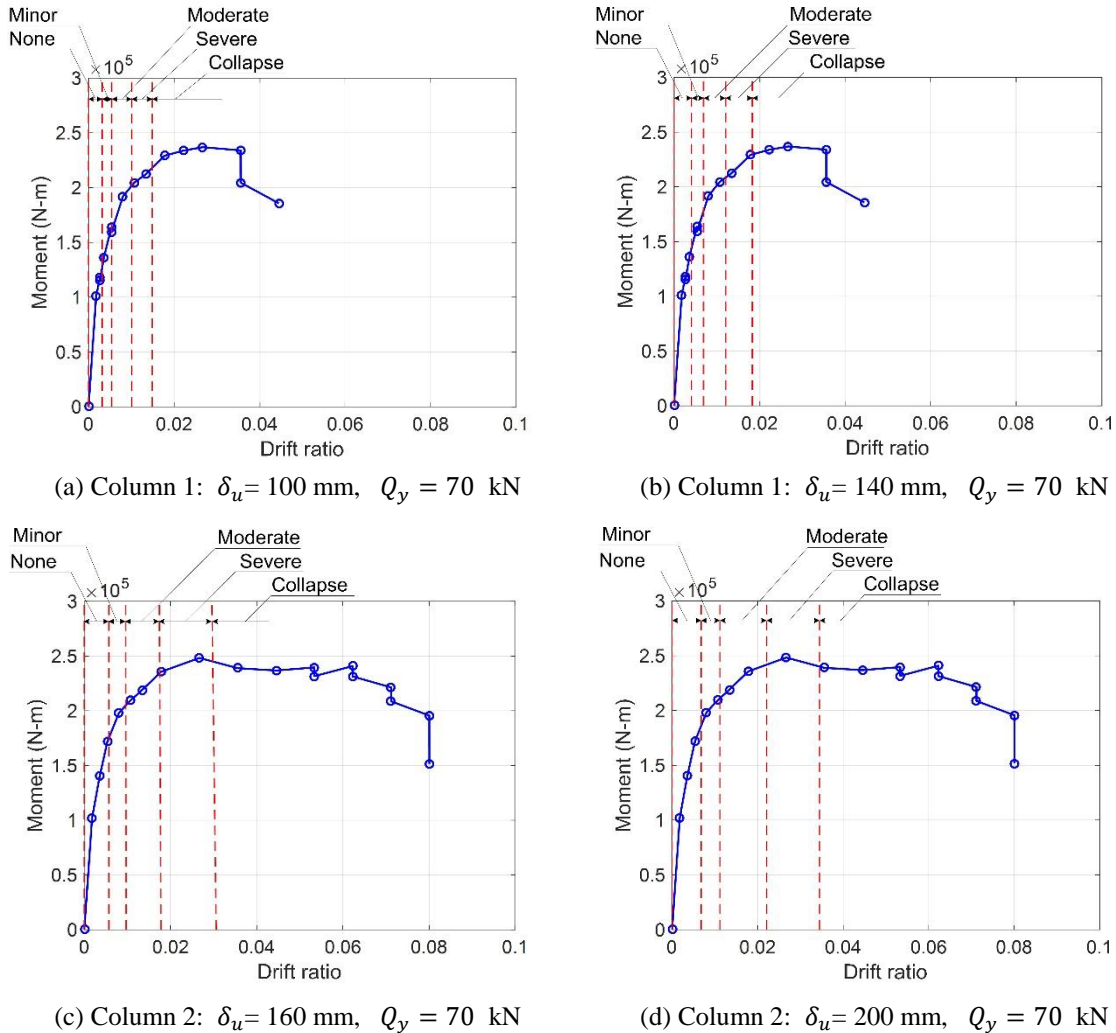


Fig. 1 Damage states variation in moment versus peak drift ratio curves of Columns 1 and 2

and the suggested method is complicated for practical applications. Therefore, using Park and Ang damage index could result in large variation of damage state ranges, which could raise the objectivity problem of the damage index in evaluating the seismic damage of structural members.

### 3. Cyclically-loaded reinforced concrete column model

In this study, local damage estimated by the Lee and Fenves plastic damage model plays an important role in establishing an objective structural damage index. In this section the plastic-damage model suggested by Lee and Fenves (1998a, 1998b) is reviewed first, then the finite element modeling method for reinforced concrete structures suggested by Lee (2001) is outlined.

### 3.1 Plastic-damage concrete model

This Lee and Fenves plastic-damage model is a widely-used nonlinear material model derived from classical plasticity and continuum damage mechanics to represent concrete-like materials under cyclic and dynamic loading (ABAQUS 2015).

In the plastic-damage model, the stress  $\boldsymbol{\sigma}$  is factored into the degradation damage,  $(1 - D)$ , and the effective stress,  $\bar{\boldsymbol{\sigma}}$

$$\boldsymbol{\sigma} = (1 - D)\bar{\boldsymbol{\sigma}} \quad (3)$$

The scalar variable  $D$  is assumed to represent the state of degradation damage on the stiffness:  $\mathbf{E} = (1 - D)\mathbf{E}_0$  where  $\mathbf{E}_0$  is the initial elastic stiffness tensor. Using the yield surface function  $F$ , the effective stress and its admissibility is defined by the following inequality equation

$$\bar{\boldsymbol{\sigma}} = \mathbf{E}_0 : (\boldsymbol{\varepsilon} - \boldsymbol{\varepsilon}^p) \in \{\bar{\boldsymbol{\sigma}} | F(\bar{\boldsymbol{\sigma}}, \boldsymbol{\kappa}) \leq 0\} \quad (4)$$

where  $\boldsymbol{\varepsilon}^p$  is the plastic strain and  $\boldsymbol{\kappa} = [\kappa_t \quad \kappa_c]^T$  is a damage variable vector consisting of two monotonically-increasing scalars: the tensile damage variable  $\kappa_t$  and the compressive damage variable  $\kappa_c$ . The factorization of the strength function into two functional forms, one for the effective stress and the other for the degradation damage variable, leads to the following damage evolution equation described with  $\mathbf{H}$ , a vector function of the effective stress and damage variable vector

$$\dot{\boldsymbol{\kappa}} = \dot{\lambda} \mathbf{H}(\bar{\boldsymbol{\sigma}}, \boldsymbol{\kappa}) \quad (5)$$

where  $\dot{\lambda}$  is a non-negative function referred to as the plastic consistency parameter.

For modeling the cyclic behavior of concrete, which has very different tensile and compressive yield strengths, it is necessary to use two cohesion variables in the yield function:  $c_t$ , a tensile cohesion variable, and,  $c_c$ , a compressive cohesion variable. The yield function in Lubliner, Oliver *et al.* (1989), which only models isotropic hardening behavior in the classical plasticity sense, is modified to include two cohesion variables as follows

$$F(\bar{\boldsymbol{\sigma}}, \boldsymbol{\kappa}) = \frac{1}{1 - \alpha} [\alpha I_1 + \sqrt{3} J_2 + \beta(\boldsymbol{\kappa}) \langle \hat{\sigma}_{max} \rangle - c_c(\boldsymbol{\kappa})] \quad (6)$$

where  $\hat{\sigma}_{max}$  denotes the algebraically maximum principal stress, and  $\alpha$  is a parameter which is evaluated by the initial shape of the yield function. The evolution of the yield function is determined by defining  $\beta$ , which is, in contrast, a constant in the original model

$$\beta = \frac{c_c(\boldsymbol{\kappa})}{c_t(\boldsymbol{\kappa})} (1 - \alpha) - (1 + \alpha) \quad (7)$$

A non-associative flow rule derived from the Drucker-Prager-type plastic potential function is used to generate the dilatancy exhibited by frictional materials

$$\dot{\boldsymbol{\varepsilon}}^p = \dot{\lambda} \left( \frac{\mathbf{s}}{\|\mathbf{s}\|} + \alpha_p \mathbf{I} \right) \quad (8)$$

where  $\|\mathbf{s}\| = \sqrt{\mathbf{s} : \mathbf{s}}$  denotes the norm of the deviatoric effective stress  $\mathbf{s}$ , and the parameter  $\alpha_p$  is chosen to give the proper dilatancy for concrete.

The experimental cyclic tests of concrete demonstrate that the degradation of stiffness from microcracking in tension and compression becomes more significant as the strain increases. The

mechanism of stiffness degradation under cyclic loading is complicated because of the opening and closing of microcracks. The crack opening/closing behavior can be modeled as elastic stiffness recovery during elastic unloading from a tensile state to a compressive state. Using a multiplicative parameter  $0 \leq s \leq 1$  on the tensile degradation variable  $D_t$ , the degradation damage variable is defined:  $D = 1 - (1 - D_c(\boldsymbol{\kappa}))(1 - sD_t(\boldsymbol{\kappa}))$ , where  $D_c$  is the compressive degradation variable. Accordingly, the total stress  $\boldsymbol{\sigma}$  is written as

$$\boldsymbol{\sigma} = (1 - D_c(\boldsymbol{\kappa}))(1 - sD_t(\boldsymbol{\kappa}))\mathbf{E}_0 : (\boldsymbol{\varepsilon} - \boldsymbol{\varepsilon}^p) \quad (9)$$

The parameter is chosen to represent the stiffness recovery as follows:

$$s(\bar{\boldsymbol{\sigma}}) = \frac{\sum_{i=1}^3 \langle \hat{\boldsymbol{\sigma}}_i \rangle}{\sum_{i=1}^3 |\hat{\boldsymbol{\sigma}}_i|} \quad (10)$$

To avoid the ill-posedness in representing the softening behavior with a model based on rate-independent plasticity, the regularization scheme based on the Duvaut-Lions viscoplastic model is applied to the rate-independent plastic strain and degradation damage variable (Lee and Fenves 1998b, Lee 2001)

$$\dot{\boldsymbol{\varepsilon}}^i = \frac{1}{\mu} (\boldsymbol{\varepsilon}^p - \boldsymbol{\varepsilon}^i) \quad (11)$$

$$\dot{\bar{D}} = \frac{1}{\mu} (D - \bar{D}) \quad (12)$$

where  $\mu$  is the viscosity parameter,  $\boldsymbol{\varepsilon}^i$  is the viscoplastic strain, and  $\bar{D}$  is a viscously regularized degradation variable. Accordingly, the stress-strain relation in Eq. (9) is restated using the new rate-dependent variables in Eqs. (11)-(12) as

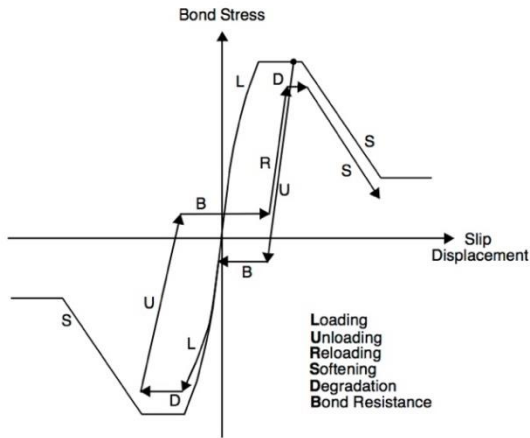
$$\boldsymbol{\sigma} = (1 - \bar{D})\mathbf{E}_0 : (\boldsymbol{\varepsilon} - \boldsymbol{\varepsilon}^i) \quad (13)$$

### 3.2 Reinforced concrete model

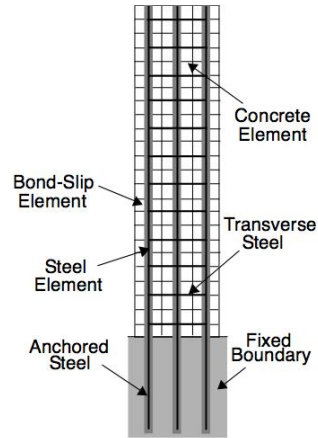
A reinforced concrete model consisting of the plastic-damage concrete, reinforcing steel bars and bond-slip link elements were suggested by Lee (2001). To reproduce the realistic reinforced concrete column behavior under cyclic and dynamic loading, a concrete model must represent initiation and localization of tensile cracking and compressive crushing damage, as well as stiffness degradation and stiffness recovery on crack closing, which is successfully implemented by the Lee and Fenves plastic-damage model (Lee and Fenves 1998a).

In this study, the modified uniaxial model proposed by Filippou, Popov *et al.* (1983) is used for the cyclic constitutive relation of longitudinal and transverse steel reinforcement. The constitutive model for the steel reinforcement is implemented in truss elements to represent reinforcing bars separately from concrete. This separated modeling provides better representation for the cracked reinforced concrete body than the so-called embedded model, because the present modeling approach can simulate more damaged states (Lee 2001). It is assumed that reinforcing bars are indirectly connected to surrounding concrete through imaginary bond-slip material, which is modeled by the discrete link described in Eligehausen, Popov *et al.* (1983). The cyclic behavior of the present bond-slip link is depicted in Fig. 2(a).

Those concrete, reinforcing bar and bond-slip models are implemented within FEAP (Talyor

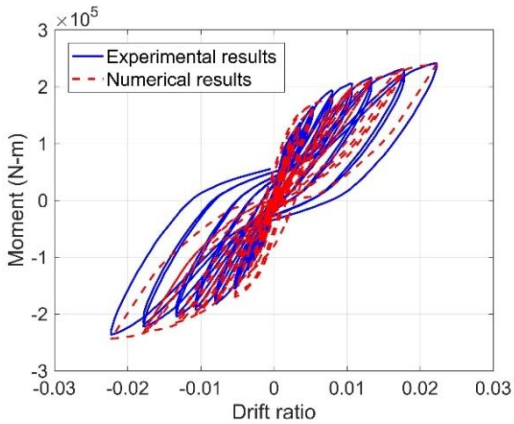


(a) Cyclic behavior of bond-slip model

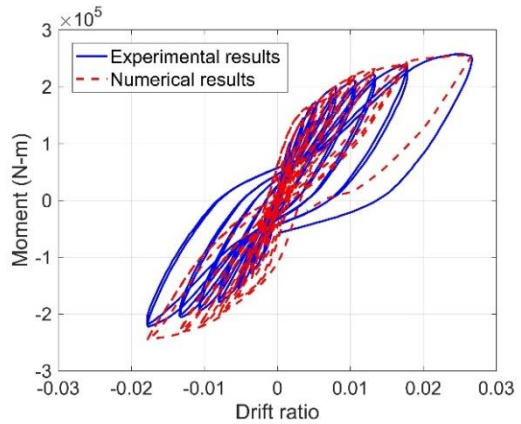


(b) Composition of reinforced concrete structural elements

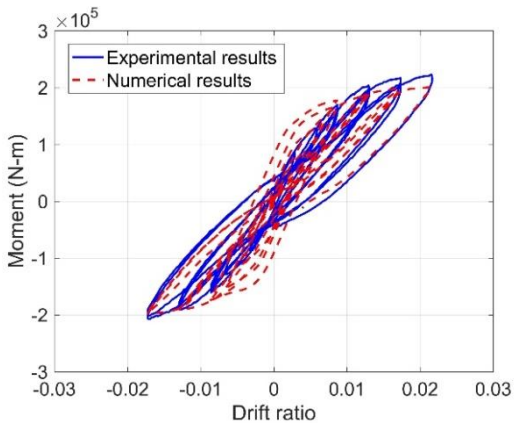
Fig. 2 Finite element model for reinforced concrete columns (Lee 2001)



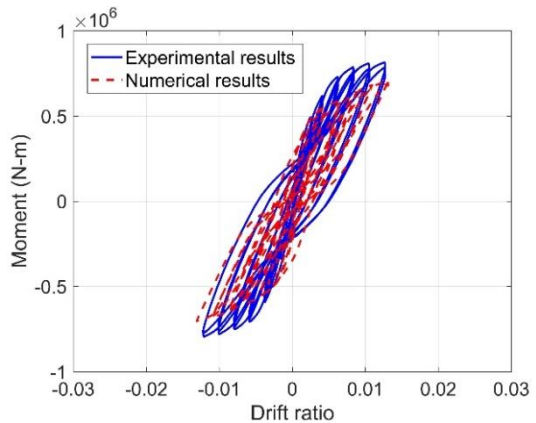
(a) Column 1



(b) Column 2



(c) Column 3



(d) Column 4

Fig. 3 Moment versus drift ratio curves from experimental tests and numerical analysis for four columns

2008), a nonlinear finite element analysis platform. Fig. 2(b) shows a reinforced concrete column model as a composition of the plane stress isoparametric element with the Lee and Fenves plastic-damage model for concrete, nonlinear truss element for rebar, and nonlinear zero-length truss element for bond-slip connection. Slip is supposed to take place only along the longitudinal direction of a reinforcing bar, and transverse directional slip is constrained by imposing large stiffness for that direction. By using the described reinforced concrete column model, the numerical simulation of nonlinear finite element analysis was performed for Columns 1 to 4 described in Section 2, subjected to displacement loading applied at the top of each column as the experimental tests.

Fig. 3 shows hysteretic moment versus drift ratio curves obtained by the quasi-static experimental tests and numerical simulation for Columns 1 to 4. For each column, the hysteresis loop from numerical analysis matched reasonably with that from the quasi-static test, although pinching phenomenon occurred in the numerical analysis. It is noted that Column 2 has slightly larger energy absorption capacity than Column 1 due to the increased confinement effect by higher transverse reinforcement ratio. From the similarity of hysteresis loops, it can be concluded that the nonlinear analysis using the Lee and Fenves plastic damage model simulates the cyclic response of columns realistically.

#### 4. New damage index based on local damage variable

Since the damage variable of the Lee and Fenves plastic-damage model in Section 3.1 gives the local damage value of a concrete column, it can be used as the fundamental information for measuring a damage level of the entire structure subject to cyclic and dynamic loading. To reasonably relate the local damage distribution to global damage levels, a new damage index should represent damage evolution stages with appropriate progress speed. In this section development of a new global damage index based on the tensile damage variable  $\kappa_t$  of the Lee and Fenves's plastic damage model is described. The suggested damage index is zoned by calibrating with the EERI damage states and their Park and Ang's damage index values to obtain the corresponding bounds of the damage states. To develop a global damage index, the following observations are made:

- 1) In each loading cycle global damage state is monotonically progressed with the increase of the peak drift ratio of a reinforced concrete column;
- 2) As a reinforced concrete column becomes more slender, the local damage spreads broader along its length.

The first observation can be justified from the results as in Fig. 1, which shows moment versus peak drift ratio curves from the column tests. It is noted that the drift ratio value itself is not appropriate to be directly used as a parameter for the global damage index, because it varies from zero to the peak value in a certain loading cycle.

While the second one is not valid in the case of plain concrete columns, where the plastic damage zone is strongly localized, in a reinforced concrete column the concrete damage is not limited within the plastic hinge zone and keeps developing along its length. This tendency becomes more intensified by the larger slenderness ratio as shown in Fig. 4, where the sectional damage ratio distribution along the height of a column is plotted. The sectional damage ratio is defined as  $[\int_{\Gamma} \kappa_t d\Gamma]_y / A$ , where  $\Gamma$  is the areal domain and  $A$  is the area at the height of  $y$  of a column.

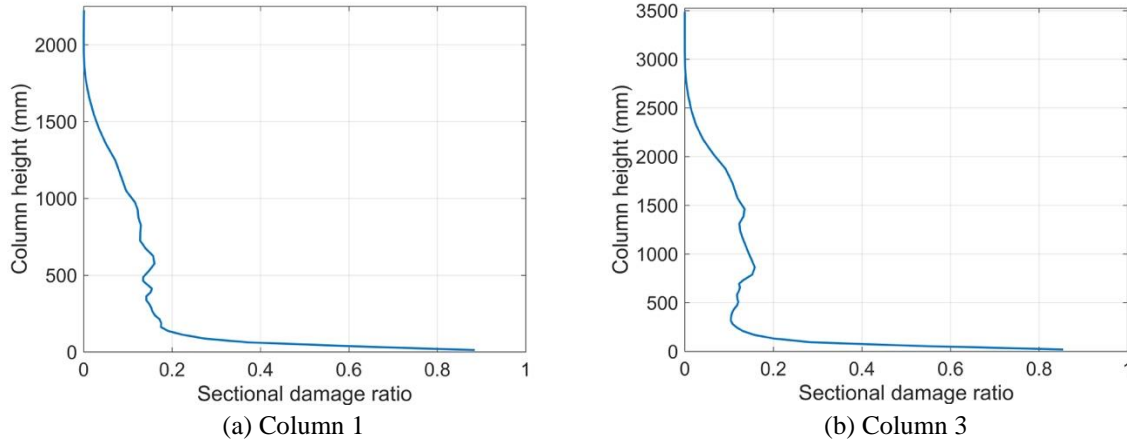


Fig. 4 Distribution of sectional damage ratio along column length at drift ratio of 2.2%

As a major damage index parameter, the volumetric damage ratio  $K_v$  is defined as

$$K_v = \frac{v \int_{\Omega} \kappa_t d\Omega}{V} \tag{14}$$

where  $\Omega$  is the volumetric domain and  $V$  is the total volume of a column. In Eq. (14), the modification factor  $v$  is introduced to account for the second observation

$$v = \min(H, nD)/H \tag{15}$$

where  $H$  is the height and  $D$  is the width (or diameter) of the column, and  $n$  is a positive real number. In the present study, the value of 6 is used for  $n$  after calibrating the column test results as in Fig. 5. Consequently, the range of the volumetric damage ratio becomes:  $0 \leq K_v \leq 1$ . It is noted that  $K_v$  is a monotonically-increasing function of the field local damage variable  $\kappa_t$ , which is also monotonically-increasing at all the points in  $\Omega$ .

Based on the first observation, the new global damage index,  $\chi$ , is proposed in the form as

$$\chi = cQ(\rho_w)K_v^q \tag{16}$$

where  $c$  is a coefficient and  $q$  is an exponent to be determined, and  $Q(\rho_w)$  is a confinement factor function of the lateral confinement reinforcement ratio,  $\rho_w$ , in percentage. The confinement factor is necessary due to lack of confinement parameters or compressive local damage variables in Eq. (14). Considering the two formulations suggested by Park and Ang (1989), of which one is shown in Eq. 1, the following formulation is suggested as the confinement factor in this study

$$Q(\rho_w) = 0.8^{\rho_w} \tag{17}$$

with the range of confinement as  $0 \leq \rho_w \leq 3$ , since it is assumed that the excessive transverse reinforcement, more than  $\rho_w = 3$ , does not provide the additional confinement.

The coefficient  $c$  is determined by setting the reference level of  $K_v$  at  $\chi = 1$  and  $Q = 1$  as  $K_{v1}$  in Eq. (16)

$$c = K_{v1}^{-q} \tag{18}$$

To determine the exponent,  $q$ , in Eq. (16), nonlinear regression is applied on the data of the drift ratio,  $\varphi$ , in percentage versus the volumetric damage ratio,  $K_v$ , from the four column tests described in Section 2, and gives the formulation as

$$K_v = (0.0628)\varphi^{0.664} \quad (19)$$

The regression result is shown with the original data in Fig. 5, where the red solid line represents the regressed curve.

Since the drift ratio is not directly used for the new damage index definition, it is necessary to set the assumed relation between  $\chi$  and  $\varphi$ , which is now the regressed drift ratio

$$\chi = \bar{c}Q(\rho_w)\varphi \quad (20)$$

where  $\bar{c}$  is a coefficient and merged into  $c$  in the following equation. Deriving the inverse relation from Eq. (19) and substituting it into Eq. (20) gives the exponent value of  $q = 1.5$  in Eq. (16)

$$\chi = cQ(\rho_w)K_v^{1.5} \quad (21)$$

where the coefficient value in the inverse function of Eq. (18) and  $\bar{c}$  is merged into the coefficient  $c$  for simplicity. By setting  $K_{v1} = 0.11$ , which is an upper bound of  $K_v$  in Fig. 5 and implies that 11% of a whole volume is completely damaged when  $\chi = 1$  and  $Q = 1$ , the coefficient  $c$  is determined as 27 by Eq. (18). Finally, the formulation, Eq. (21), of the proposed damage index for the global damage level of a reinforced concrete column becomes

$$\chi = 27(0.8^{\rho_w})K_v^{1.5} \quad (22)$$

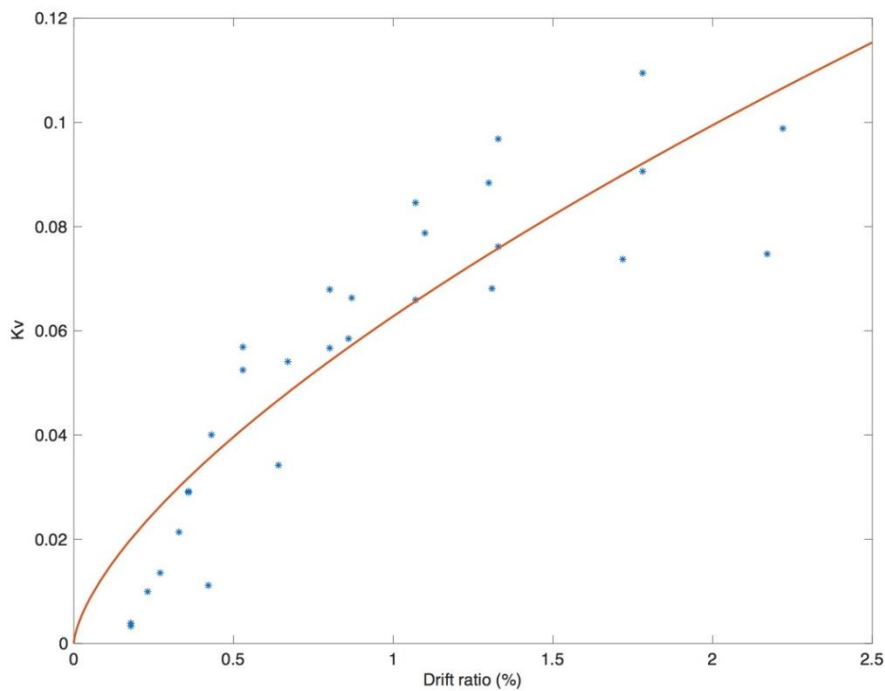


Fig. 5 Nonlinear regression on the volumetric damage ratio ( $K_v$ ) versus drift ratio

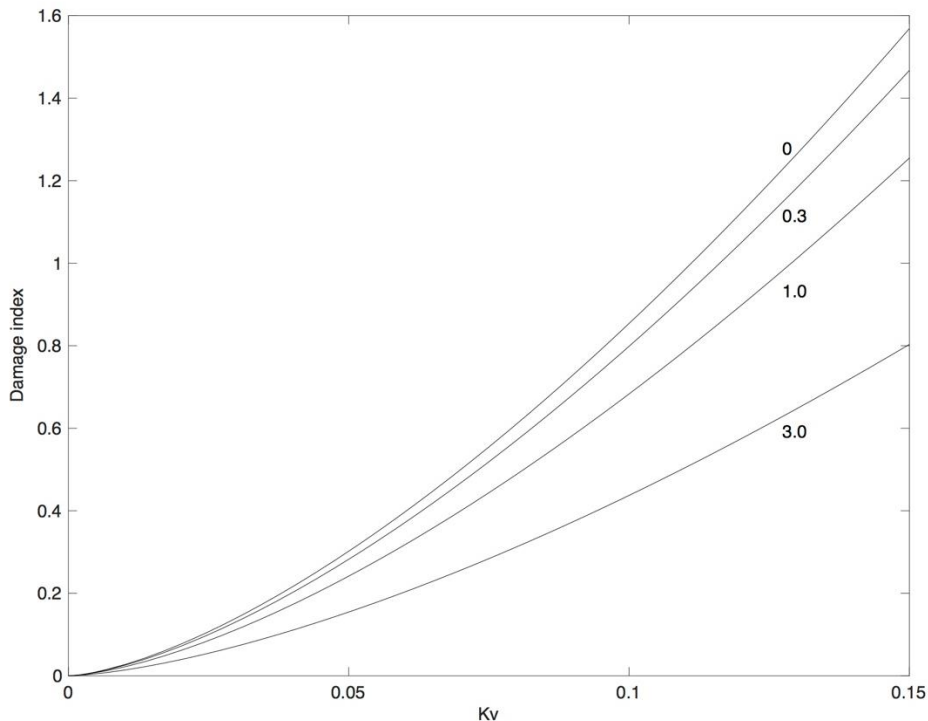


Fig. 6 Damage index ( $\chi$ ) versus the volumetric damage ratio ( $K_v$ ) with four lateral confinement reinforcement ratio values ( $\rho_w = 0, 0.3, 1.0, 3.0$ )

Fig. 6 shows four curves of the damage index function in Eq. (22) for four different lateral confinement ratios,  $\rho_w$ .

While the theoretical maximum of the proposed damage index,  $\chi$ , is the coefficient  $c$ , which is 27 in Eq. (22), its range is expected to be from 0 to 1 in practical use as observed in Fig. 7, where the proposed damage index curves are plotted from the numerical simulation results for the four column tests described in Section 2. As the peak drift ratio is increased under cyclic loading as shown in Fig. 3, the damage index values are monotonically increased. It is also observed that all damage index curves but Column 1 curve fail to reach higher index level than 0.7 because the simulation is terminated due to numerical instability in highly nonlinear region.

The proposed damage index curve is compared with Park and Ang's one for the same numerical simulation result of Column 1 in Fig. 8. The index values are normalized to their maximum values. The Park and Ang damage index gives a smooth exponential-like curve because it is based on the apparent values and external energy dissipation computation. On the other hand, the proposed damage index shows relatively fast progress of the global damage in the initial stage, and its slope becomes lower after about the drift ratio of 0.5%, when concrete cracking damage is significantly developed and nonlinearity of reinforcing bars begins to dominate the overall behavior of a reinforced concrete column. Regardless of the difference in the curve shape, both damage indices show the monotonically increase function for the peak drift ratio value, which implies that the proposed damage index is valid as a damage index function.

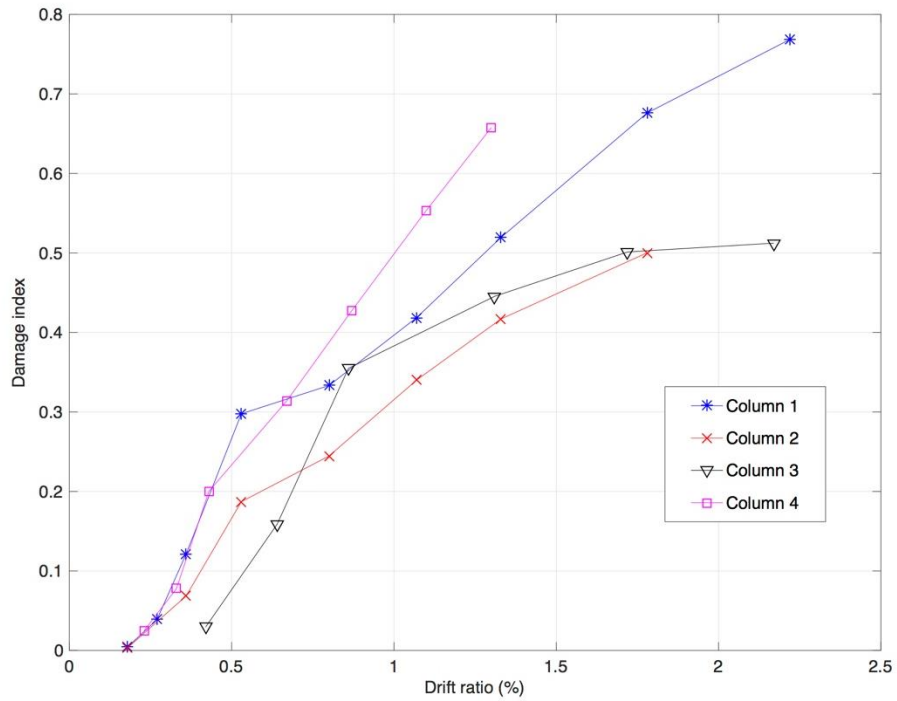


Fig. 7 Damage index ( $\gamma$ ) versus drift ratio curves for four tested columns

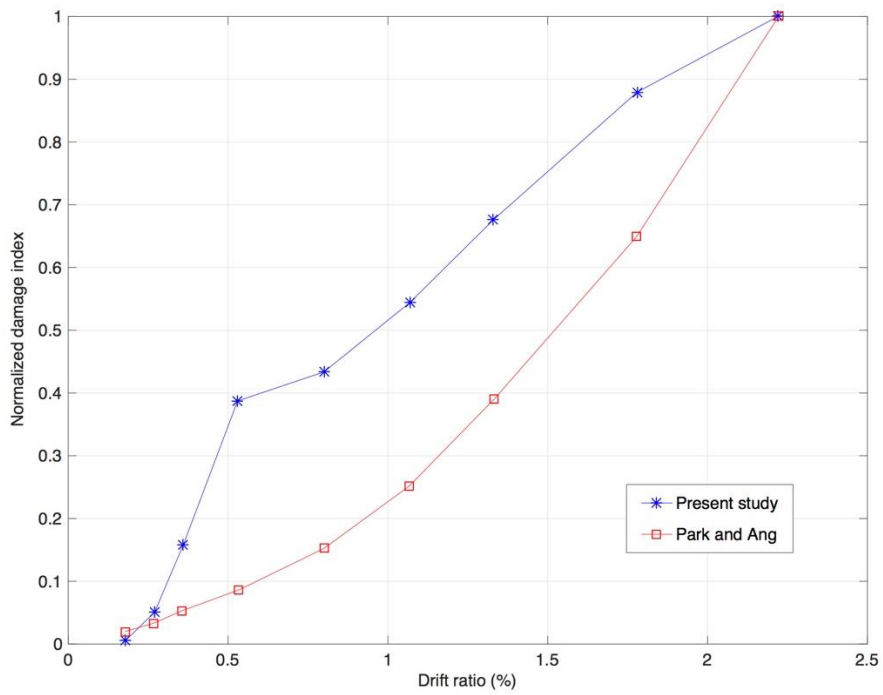


Fig. 8 Comparison of normalized damage indices versus drift ratio curves for Column 1

Table 3 Drift ratio bounds of tested columns for each EERI damage state

EERI damage state	Minor	Moderate	Severe	Collapse
Park and Ang damage index bounds ( $D_{PA}$ )	0.1	0.2	0.5	1.0
Column 1	0.41	0.69	1.21	1.83
Column 2	0.57	0.97	1.78	3.06
Column 3	0.61	0.95	1.70	2.40
Column 4	0.35	0.58	0.99	1.42

Table 4 Damage index ranges for EERI damage states

EERI damage state	None	Minor	Moderate	Severe	Collapse
Range of damage index ( $\chi$ )	0.0 ~ 0.1	0.1 ~ 0.3	0.3 ~ 0.5	0.5 ~ 0.7	> 0.7

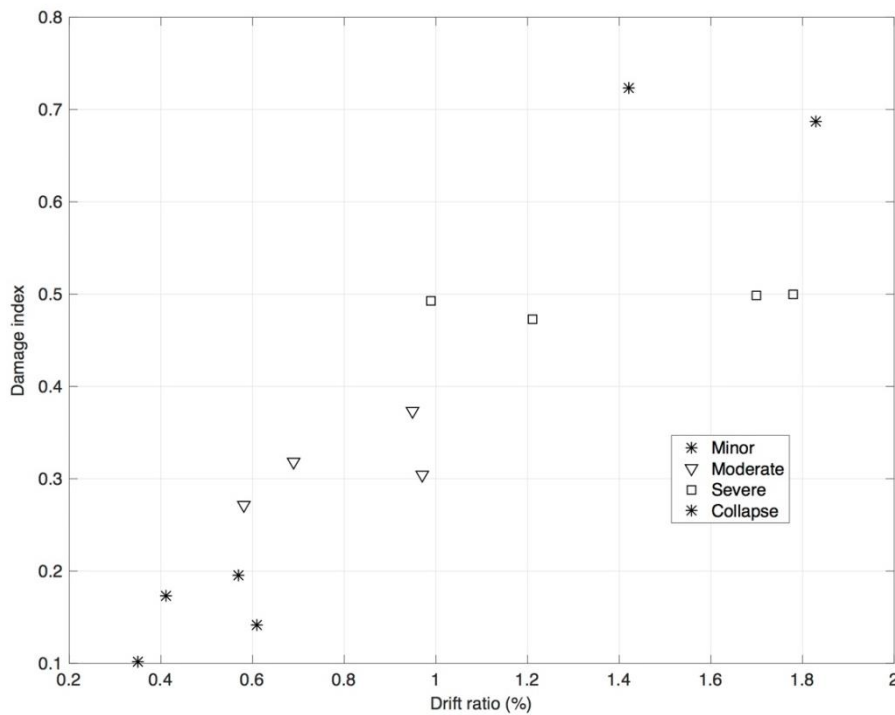


Fig. 9 Damage index ( $\chi$ ) points at drift ratios of damage state bounds for four tested columns

## 5. Application in seismic fragility analysis

### 5.1 Determination of damage state bounds

To use the developed damage index for seismic fragility analysis of reinforced concrete columns, it is necessary to establish the relationship between the damage index and damage states.

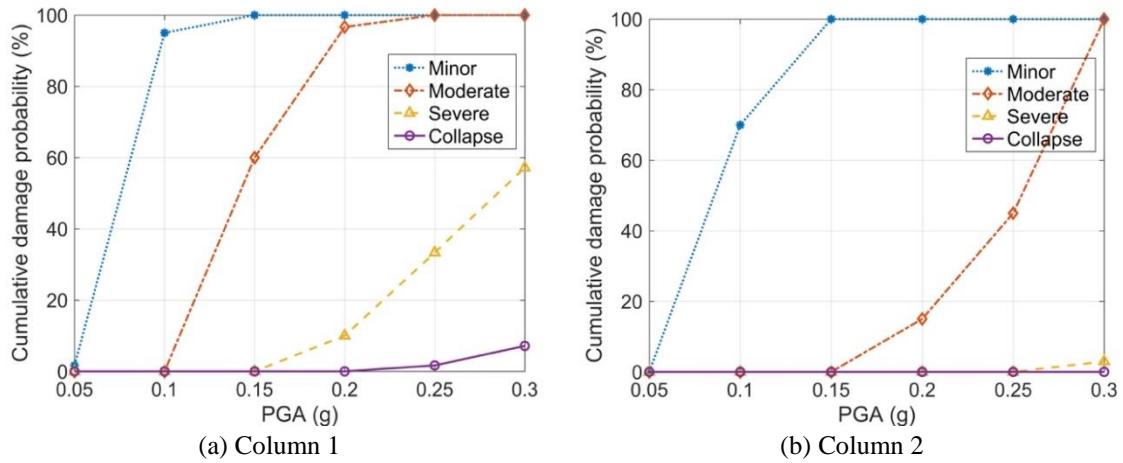


Fig. 10 Fragility curves for (a) Column 1 and (b) Column 2

In the present study the five-level EERI damage states are used for the seismic fragility analysis. The Park and Ang damage index zoned by the EERI damage states can be used to assign a value from the proposed damage index to a corresponding damage state.

The lower bounds of peak drift ratio for each EERI damage state is obtained by calculating the Park and Ang damage index based on the experimental column tests data as shown in Table 3. The values in the row of the Park and Ang damage index bounds in Table 3 are obtained from Table 1.

Assuming that the numerical model realistically simulates the experiments, the proposed damage index,  $\chi$ , at each lower bound peak drift ratio in Table 3 is computed and plotted in Fig. 9. It is observed that the damage index values for the certain damage state are well agreed each other. From this observation, the ranges of the proposed damage index for the five EERI damage states are suggested as in Table 4.

## 5.2 Seismic fragility evaluation

Fragility curve represents the conditional probability as

$$P_{ij} = P[S \geq S_i | A_j] \quad (23)$$

where  $S$  is the damage state,  $S_i$  is the  $i$ -th level of the damage state, and  $A_j$  is the  $j$ -th earthquake level. In the present study the damage state is determined based on the suggested ranges of the newly proposed damage index. The peak ground acceleration (PGA) values are used for the magnitude of earthquake. Fig. 10 shows seismic fragility curves obtained from nonlinear finite element time-history analyses and damage assessment of Columns 1 and 2. The seismic analysis was conducted with 360 artificial ground motions generated from the target spectral density of earthquake (Shinozuka and Deodatis 1991). Various site conditions are implicitly incorporated in those artificial ground motions. The PGA of the ground motion ranges from 0.05 g to 0.30 g with increment of 0.05 g, where g is the gravitational acceleration. The calculation of seismic fragility was based on Monte-Carlo simulation method with the 360 random ground motions. Although the number is not enough to model the significant uncertainty of input ground motions, it can be considered that the fragility curves of Fig. 10 represent the trend of damage probability with

respect to the intensity of ground motions reasonably well.

In contrast to Column 1, Column 2 was designed with high transverse reinforcement ratio for seismic enhancement. The fragility curves show that the probability of collapse or severe damage state is much higher in Column 1 than Column 2 if PGA is greater than 0.2 g. This result can be attributed to the relatively higher ratio of transverse reinforcement for Column 2. The result of lower seismic fragility of Column 2 is consistent with the shift of damage state ranges to higher drift zones compared to the damage state ranges of Column 1, as illustrated in Fig. 1.

## 6. Conclusions

A structural damage index for seismic fragility analysis of reinforced concrete columns is suggested as a single monotonically-increasing function of the volume weighted average of local tensile damage distribution, which is computed by the Lee and Fenves plastic-damage model. In contrast to the response-based damage index, the proposed damage index is well-defined in the form of a single monotonically-increasing function of the volume weighted average of local damage distribution, and provides the necessary computability and objectivity because it does not require to compute the ultimate displacement and yield strength. The nonlinear regression of experimental reinforced concrete column test data is used to derive the damage index function, which enhances its representability for the global damage progress of a structure.

It is observed that the developed damage index gives a consistent range of values for each EERI damage state of the tested columns. This observation shows that the present damage index can be appropriately zoned to be used in seismic fragility analysis. The demonstration of its successful application in the seismic fragility evaluation of two reinforced concrete columns validates the proposed damage index. It is expected that the coefficient and exponent parameters of the damage index function are improved by using the same procedure presented with more test data. The damage index form of a single monotonically-increasing function is also expected to be utilized for fragility function derivation to effectively reduce the necessary number of simulations.

Although damage caused by bond-slip and yield of a reinforcing bar is indirectly taken into account through the plastic-damage evolution equations in the proposed damage index, further studies are needed to precisely reflect compressive damage of concrete, inelastic buckling of reinforcing bars and bond-strength deterioration on the damage index.

## Acknowledgments

This work was supported by the research program of Dongguk University, 2014. This research was partially supported by the Basic Science Research Program through the National Research Foundation of Korea [2014R1A1A1006419].

## References

- ABAQUS (2015), ABAQUS Theory Manual, Dassault Systemes, RI, USA.
- Amziane, S. and Dubé, J.F. (2008), "Global RC structural damage index based on the assessment of local material damage", *J. Adv. Concrete Tech.*, **6**(3), 459-468.

- Andre, J., Beale, R. and Baptista, M. (2015), "New indices of structural robustness and structural fragility", *Struct. Eng. Mech.*, **56**(6), 1063-1093.
- Azhdary, F. and Shabakhty, N. (2014), "Performance based design and damages estimation of steel frames with consideration of uncertainties", *Tehnički Vjesnik*, **21**(2), 351-358.
- Dumova-Jovanoska E. (2000), "Fragility curves for reinforced concrete structures in Skopje (Macedonia) region", *Soil Dyn. Earthq. Eng.*, **19**, 455-466.
- EERI (1994), "Expected seismic performance of buildings", Publication SP-10, Earthquake Engineering Research Institute, Oakland, CA, USA.
- Eligehausen, R., Popov, E.P. and Bertero, V.V. (1983), "Local bond stress-slip relationships of deformed bars under generalized excitations", EERC Report 83-23, Earthquake Engineering Research Center, University of California, Berkeley, CA, USA.
- Filippou, F.C., Popov, E.P. and Bertero, V.V. (1983), "Effects of bond deterioration on hysteretic behavior of reinforced concrete joints", EERC Report 83-19, Earthquake Engineering Research Center, University of California, Berkeley, CA, USA.
- Hadzima-Nyarko, M., Morić, D. and Španić, M. (2014), "Spectral functions of RC frames using a new formula for damage index", *Tehnički Vjesnik*, **21**(1), 163-171.
- Jiang, H.J., Chen, L.Z. and Chen, Q. (2011), "Seismic damage assessment and performance levels of reinforced concrete members", *Procedia Engineering; the Twelfth East Asia-Pacific Conference on Structural Engineering and Construction*, **14**, 939-945.
- Koh, H.M., Lee, J. and Kang, J.W. (2003), "Seismic damage evaluation of reinforced concrete pier based on a plastic damage model", *J. Kor. Soc. Civil Eng.*, KSCE, **23**(5), 1029-1039.
- Lee, J. (2001), "Damage analysis of reinforced concrete columns under cyclic loading", *KCI Concrete J.*, **13**(2), 67-74.
- Lee, J. and Fenves, G.L. (1998a), "Plastic-damage model for cyclic loading of concrete structures", *J. Eng. Mech.*, ASCE, **124**(8), 892-900.
- Lee, J. and Fenves, G.L. (1998b), "A plastic-damage concrete model for earthquake analysis of dams", *Earthq. Eng. Struct. Dyn.*, **27**, 937-956.
- Liang, H., Wen, Y.K. and Foliente, G.C. (2011), "Damage modeling and damage limit state criterion for wood-frame buildings subjected to seismic loads", *J. Struct. Eng.*, **137**(1), 41-48.
- Lublinter, J., Oliver, J., Oller, S. and Onate, E. (1989), "A plastic-damage model for concrete", *Int. J. Solid. Struct.*, **25**(3), 299-326.
- Park, Y.J. and Ang, A.H-S. (1985), "Mechanistic seismic damage model for reinforced concrete", *J. Struct. Eng.*, ASCE, **111**(4), 722-39.
- Shinozuka, M. and Deodatis, G. (1991), "Simulation of stochastic processes by spectral representation", *Appl. Mech. Rev.*, **44**(4), 191-204.
- Shinozuka, M., Feng, M.Q., Kim, H., Uzawa, T. and Ueda, T. (2003), "Statistical analysis of fragility curves", Report No. MCEER-03-0002, MCEER, Buffalo, NY, USA.
- Sinha, R and Shiradhonkar, S.R. (2012), "Seismic damage index for classification of structural damage-closing the loop", *15th World Congress on Earthquake Engineering*, Lisbon, Portugal, September.
- Taylor, R.L. (2008), *FEAP: A Finite Element Analysis Program*, University of California, Berkeley, CA, USA.
- Teran-Gilmore, A. and Jirsa, J.O. (2005), "A damage model for practical seismic design that accounts for low cycle fatigue", *Earthq. Spectra*, **21**(3), 803-832.
- Vielma, J.C., Barbat, A.H. and Oller, S. (2008), "An objective seismic damage index for the evaluation of the performance of RC buildings", *14th World Congress on Earthquake Engineering*, Beijing, China, October.